A Combined Ensemble Model (CEM) for a Liver Cancer Detection System

T. Sumellika[1], Prof R. Satya Prasad[2]
Research Scholar, Dept of CSE, Acharya Nagarjuna University, Nagarjuna Nagar-522510, Andhra Pradesh, India[1]
Department of Computer Science & Engineering, Acharya Nagarjuna University,
Nagarjuna Nagar-522510, Andhra Pradesh, India[2]

***Abstract*—The liver is one of the most important organs in the human body. The liver's proper function is critical for overall health, and liver diseases or disorders can have serious consequences. Liver cancer is also known as hepatic cancer, which is divided into various types of cells that belong to the cancer. The most common type of liver cancer is hepatocellular carcinoma (HCC). HCC is one of the most common types of liver cancer that can affect up to 85% of people worldwide. Early detection of liver cancer is essential in healthcare because it increases the chances of successful treatment and patient outcomes. Many researchers have developed models that help detect and diagnose liver cancer. The first step in detecting liver cancer is identifying people at a higher risk. Chronic hepatitis B or C infection, cirrhosis, heavy alcohol use, obesity, and exposure to certain chemicals and toxins are all risk factors. This paper is mainly focused on detecting the cancer-affected regions that occur in the liver. In this paper, a combined ensemble model (CEM) for a liver cancer detection system is developed to find and detect liver cancer and liver disorders in their early stages. A pre-trained model, RESNET50 with transfer learning, is used to obtain the features from the pre-trained model—an advanced preprocessing technique involved in filtering the noise from input CT scan images. A hybrid feature extraction (HFE) technique also gets significant elements from the input CT scan images. Finally, the proposed CEM combines an Extreme Gradient Boosting (EGB) algorithm with a Recurrent Neural Network (RNN) that focuses on detecting the abnormal cancer cells present in input CT scan images. The performance of the CEM shows a high accuracy of 98.48% with a 10% high detection rate. Previously, it was 88.12%.**

Keywords*—Liver Cancer; Hepatocellular Carcinoma (HCC); Combined Ensemble Model (CEM); RESNET50; Extreme Gradient Boosting (EGB); Recurrent Neural Network (RNN)

I. INTRODUCTION

Cancer is a most complex diseases characterized by unrestricted cell growth and division in the body [1]. It is a significant public health concern worldwide and can affect almost any body part. Cells in the body normally grow, divide, and die in a controlled manner [2]. The body's genetic instructions tightly control this process. When this control is disrupted, cells can divide and grow uncontrollably, forming a tissue mass called a tumor. Tumors of two types, such as benign or malignant, Benign is non-cancerous, which is not more dangerous than malignant. Malignant is more dangerous because it is cancerous and spreads very quickly to all the body parts [3] [4]. The process of converting healthy cells into cancerous cells is known as carcinogenesis. Usually, it involves DNA alterations in the cell. These alterations can be brought on by a genetic predisposition, viral infections, to carcinogens (such as tobacco smoke or certain chemicals). The kind and stage of a cancer diagnosis can have a significant impact on the symptoms. Common symptoms include sudden weight loss, exhaustion, pain, skin changes, chronic coughing or hoarseness, lumps or masses, and altered bowel or bladder habits [5] [6]. Physical examinations, imaging tests, and laboratory testing are commonly used to diagnose cancer. Effective therapy depends on early discovery.

Image processing is an essential domain in detecting and diagnosing liver cancer. These models assist medical professionals in early cancer detection and treatment planning by extracting meaningful information from CT scans, MRIs, or ultrasound images [7]. Medical imaging, blood tests, and sometimes tissue biopsy are used to detect liver cancer. Early detection is critical for successful treatment and outcomes. A complete medical history taking into account risk factors such as alcohol use, hepatitis infection, and family history. They will also conduct a physical exam to look for signs of liver abnormalities like enlargement or tenderness [8] [9]. Several tests are available to aid in detecting and diagnosing liver cancer cells in CT scan images [10] [11]. Deep Learning (DL) is essential in detecting complex cancer patterns in liver CT scan images. Fig. 1 shows the sample liver lesions present in CT scan images.

This paper introduced the pre-trained model, such as ResNet-50, extracts accurate features from CT scan samples. Transfer learning with pre-trained models can significantly improve the proposed model's performance, particularly for limited labeled data. Denoising techniques are used in many image processing techniques to process CT scan images. In conjunction with various denoising filters, this paper removes noise from input CT scan images. Gray-level run-length Matrix (GLRLM) and region-based features were used to improve feature extraction.

A. Contributions of this Work

1) By integrating the distinct models, CEM is usually higher in forecasting because it consists of many basic models. Every model used in this work offers benefits while working on the proposed approach.

2) Complex interactions between many clinical and genetic variables are frequently involved in identifying liver cancer. CEM can more accurately forecast outcomes by

capturing these complex interactions by combining many modeling methodologies.

3) The proposed model uses the Pre-trained model RESNET50 to get the accurate cancer disease patterns in the given samples.

4) An interesting features are obtained by using the hybrid feature extraction (HFE) that helps to improve the performance of final outcomes.

II. Literature Survey

Kim et al. [12] proposed a one-sided ANOVA approach for extracting the feature set for accurate disease detection using a feature (aptamer) array. For 80 liver cancer patients and 310 healthy people, the proposed approach combined AI with 10-fold cross specifications verified by aptamer array response. The proposed ANOVA approach has an accuracy of about 93.6% for ten features, which is 3.51% higher than the single-way method. Ahmad et al. [13] proposed a new approach called DBN-DNN, which can fine-tune the proposed DNN approach. An advanced pre-processing technique improves performance by employing an active contour technique based on liver features that store memory and measure time. The evaluation result shows that the proposed approach's performance on test images achieved a Dice score of 95.34%, which is high, compared to existing models. Balagourouchetty et al. [14] developed a CAD system for diagnosing liver diseases. The proposed method uses an ensemble FCNet classifier to classify hepaticae lesions based on several significant factors obtained from GoogleNet-LReLU transfer learning approaches. The proposed approach is a fully connected layer that includes classification and extraction using the inception layer and is combined with the ReLU activation function. Finally, the variety is based on six different types of liver diseases, and it is highly accurate. Yamakawa et al. [15] developed a new model for detecting tumors in the liver. The proposed method combines CNN with VGGNet to classify the four types of tumors based on the affected regions. The dataset contains 988 images representing various cases. When combined with CADx, the proposed method predicts liver cancer tumors with an accuracy of 94.56%, which is a high detection rate. Aslam et al. [16] presented an integrated learning model that combines image processing techniques and deep learning (DL) approaches to detect early-stage liver cancer tumors. The proposed model also employs the ResUNet, the most advanced model, to achieve better results. The dataset includes 100 CT scan liver tumor images from various patients. Finally, the proposed approach's accuracy is around 99.67%, and its F1-score is 94.8%, which is high compared to other systems in this paper. Shukla et al. [17] presented the automated liver tumor detection model from MRI scan images. The proposed approach divides the concave surfaces combined with geodesic active contour. The author introduced the Cascaded Fully CNN approach to segment the tumor region from the input sample. The training process reduces the error rate for liver segmentation. The final liver tumor analysis for the proposed approach is to obtain 94.56% accuracy and 88.89 Sec for computation of liver analysis. Sanyal et al. [18] presented a new model for detecting NAFLD based on the stage of liver disease. The proposed approach provided clear information about the liver status and stage in the early stages of the disease. As a result, this approach offers the default disease information that aids in detecting and diagnosing NAFLD. Li et al. [19] investigated NAFLD using various methodologies. Zhou et al. [20] proposed NAFLD for the detection of liver cancer. The author discussed about various models that helps to diagnose the cancer cells in liver. Marengo et al. [21] presented a new model for detecting HCC, a type of common liver cancer. Other factors, such as type 2 diabetes, NAFLD, and obesity, contribute to the rapid growth of HCC. It is a rapidly spreading cancer in the general population that should be detected in its early stages. The author discussed several techniques and methods for treating HCC and devised a limited solution. Sun et al. [22] talked about a variety of liver diseases. The author concentrated on detecting obesity-related health issues and their consequences. According to epidemiological studies, obesity is the root cause of various cancers. Obesity is strongly linked to other liver diseases such as NAFLD, NASH, and cancer. Kwon et al. [23] introduced a method for segmenting liver CT scan images using DL. The author wishes to identify additional factors influencing liver cancers based on human activities and habits. Manjunath et al. [24] presented a DL approach for detecting liver disease based on tumors growth. The tumor images are collected online and classified into Metastasis and Cholangiocarcinoma. The proposed approach gets better accuracy with 97.89% and a dice score of 98.23%. Lakshmipriya et al. [25] compared various DL algorithms based on classification, segmentation, and medical details of liver diseases. The author discussed different DL algorithms and found new challenges from the existing algorithms. Piyush Kumar Shukla et al. [26] presented an automated liver disease detection system that finds the tumors and lesions in the MRI images belonging to abdomen images that are gathered from 3D-related abhorrent and shape-based model results. The proposed approach combined with geodesic active contour analysis to find the different liver regions in the body. Finally, the training approach reduces the error rate by using the CFCNs to detect the segmented tumor image. In the final step, the segmentation approach obtained a tumor detection accuracy of 94.67% with a computation time of 17 seconds for one photo. The DL technique, which identifies liver tumors from CT scan pictures, was first presented by Heng Zhang et al. [27]. The CNN model was employed to segment CT scan images. Based on experimental results, comparisons between several segmentation approaches are presented. The automated KMC method, which offers a region-based growth strategy to locate the tumor region and display tumor grades, was proposed by Liping Liu et al. [28]. The deficiencies belong to blood vessels in the portal venous phase (PVP) based on the poor density of the liver CT scan pictures. In the last stage, patients with 26.67% having low blood deposition effect and 54.34% having high blood were discovered. Nayantara et al. [29] introduced the effective segmentation that detects liver diseases accurately on CT scan images. The author analyzed several DL algorithms that find liver diseases accurately. Zhang et al. [30] presented the diagnosis of liver diseases using Dl algorithms. Mubashir Ahmad et al. [31] developed the patch-based DL algorithm that segments the liver CT scan images using SAE. The proposed approach processes every pixel of the image and finds the accurate patches of initialize

the liver disease-affected regions. The preprocessing method improved the images and created overlapping patches from each one, which were then fed into the SAE to extract features. In the last step, the classification is used to classify the affected regions based on the feature extraction. The proposed approach obtained the dice score similarity up to 97.23%, which shows high accuracy. Manoj Kumar et al. [32] proposed a comparative study that finds the overall liver disease patients based on three stages. The preprocessing technique min-max normalization is applied, and in the second step, the PSO feature extraction is used to extract the significant data from the input CT scan images and improve the disease detection rate. Li et al. [33] proposed a novel approach that detects liver cancer from liver CT scan images. Two datasets, such as MICCAI 2017 and 3DIRCADb data sets, are used for evaluation. The proposed approach focused on detecting the cancer-affected regions by using segmentation with the FCNN model and UNet (H-DenseUNet) that effectively extract the hybrid feature fusion layer. The comparison between several algorithms shows the proposed approach obtains good outcomes. Amita Das et al. [34] introduced the WGDL approach for detecting cancer lesions using CT scan images. The input CT scan images are separated using watershed segmentation and GMM to divide the cancer lesion. Finally, the DNN is used for classification based on segmentation outcomes. Anandan et al. [35] presented the enhanced filtering approach called NMADF that helps filter the input CT scan images. The proposed approach uses the two-fold segmentation that segments the liver cancer images. The canny edge detection approach is used as a preprocessing technique—finally; the improved DNN approach is used to classify liver cancer images. The results show the better performance of the proposed approach compared with existing models.

A. Limitations of Existing Models

1) The existing model requires massive training data to solve the sample imbalance.

2) There needs to be more accurate classification of normal and cancerous samples.

3) The existing models require high-quality images to detect accurate results.

4) There must be more issues in finding the accurate affected region in the given sample.

III. Dataset Description

The dataset was obtained from Kaggle and contains CT scan images related to contrast and patient age. The default viewpoint is to find various image textures tested for analyzing trends in CT scan images and statistical patterns. It features strongly correlated with these traits and possibly builds simple tools for automatically classifying these images when they have been misclassified. The total images used for training is 500 and testing is 500 CT scan liver images. The size of image in dataset is 500 x 500 width and height and size is 5-6 MB. The sample datasets with different types of images are shown in Fig. 1. All the images are in same size and pixel rate.

A. RESNET50 (Pre-Trained Model)

A common and practical approach in medical image analysis is the ResNet-50 model for cancer cell detection. ResNet-50 is deep convolutional neural network (DCNN) architecture with great success in image classification and object detection. When used to detect cancer cells, it can aid in identifying and classifying cancerous cells in medical images such as histopathology slides or radiological scans. ResNet-50 comprises 50 Convolutional layers connected by skip connections (residual blocks). The ResNet-50 weights were fine-tuned on a liver cancer cell dataset using popular deep-learning libraries such as TensorFlow. On the training data, train the ResNet-50 model with appropriate loss functions such as binary cross-entropy or focal loss for binary classification (cancerous or non-cancerous). To attain the highest validation set performance, track and modify hyper parameters like learning rate and batch size. To avoid over-fitting, techniques such as early stopping are used. If necessary, the post-process approach is used to predict to remove noise or refine the detected cancerous regions. The overall architecture of RESNET 50 is explained in Fig. 3. The input image and final output is obtained after processing all layers.

B. Pre-processing and Noise Removal

Pre-processing is essential in removing noise from input liver CT scan images. This paper combines an advanced pre-processing technique with Iterative Reconstruction (IR) and Anisotropic Diffusion (AD). It is beneficial for removing noise and improving image quality and diagnostic accuracy in CT (computed tomography) scan images. Various noise reduction techniques can be used depending on the specific noise characteristics and the image processing goals. Fig. 2 and Fig. 5 shows the input and output of the image selected from dataset.

C. Iterative Reconstruction (IR)

Iterative reconstruction is a computational technique used in medical imaging to improve image quality and reduce radiation exposure, particularly in CT (computed tomography) scans. It is an alternative to traditional filtered back projection (FBP). It is a simpler and faster method but may result in lower-quality images, mainly when data is limited, or measurements are noisy. Iterative reconstruction algorithms can address these issues by refining the vision iteratively based on the acquired data and a mathematical model of the imaging process. A CT scanner captures a series of X-ray projections as it rotates around the patient. These projections are different angles of CT-Scan attenuation through the patient's body. The iterative reconstruction process estimates the patient's internal structures, usually a simple or uniform image. The initial image generates CT-Scan projections as if the image were actual. This step uses a mathematical model that accounts for the CT-Scan attenuation properties of the tissues being imaged.

x: The true underlying image we want to reconstruct.

y: The acquired data (e.g., projection data in CT imaging).

R: The reconstruction operator that maps the image x to the acquired data y.

ϵ: The noise or error in the data.

The iterative reconstruction process can be represented mathematically using the following equation:

$$y = R(x) + \in$$

The goal is to find the best estimate x_k of the true image x iteratively minimizing the variance among the acquired and estimated data $R(x_k)$. this is typically done by solving the optimization issue at every iteration:

$$x_{k+1} = \text{argmin}_x\{||y - R(x)||^2 + \lambda\, \Phi(x)\}$$

$||y - R(x)||^2$ Represents the data fidelity term, $\Phi(x)$ is a regularization term that enforces some desired properties on the reconstructed image, such as smoothness or sparsity.

λ is a regularization parameter that controls the trade-off between data fidelity and regularization.

D. Anisotropic Diffusion (AD)

Anisotropic Diffusion (AD) is a method for edge-preserving smoothing in image processing. When used to enhance or denoise photos while maintaining structural integrity, it is especially helpful. AD can be used in the context of medical imaging to enhance the visibility of pertinent features, such as scans showing malignancy. Anisotropic diffusion is based on the principle of performing diffusion in a way that is less noticeable in homogenous regions and more evident along the image's borders. This reduces noise while maintaining significant edges and structures.

The AD equation is represented as:

$$\frac{\partial I}{\partial t} = \nabla.\,(c(||\nabla I||)\nabla I)$$

I is the image intensity

∇ is the gradient operator

$||\nabla I||$ is the magnitude of the gradient,

$c(||\nabla I||)$ is the diffusion coefficient.

t is the time.

Based on the gradient's magnitude, the diffusion coefficient $c(||\nabla I||)$ is a function that establishes the appropriate amount of diffusion at each location. The role that is applicable as:

$$c(||\nabla I||) = e^{-(\frac{||\nabla I||^2}{K^2})}$$

The amount of diffusion is controlled by the parameter K in this case. Greater diffusion is permitted by smaller K values, while greater K values better maintain edges. Iteratively solving the equation over the image is done until the desired degree of smoothing is attained. The goal of the procedure is to maintain edges and fine structures while smoothing the image more over homogeneous areas. Anisotropic diffusion can be used to improve the visibility of significant characteristics in cancer images, which will facilitate medical experts' analysis and interpretation of the images.

E. Gray-Level Run-Length Matrix (GLRLM)

A popular texture analysis technique in medical image processing is the GLRLM. CT scan images are analyzed for a variety of purposes, including cancer detection. GLRLM provides texture pattern information by quantifying the distribution of grey-level runs in an image. The GLRLM describes the correlations between pixel intensities along various directions and is commonly obtained from the co-occurrence matrix. Features that characterize an image's texture can be extracted using the GLRLM and used for classification or other analysis purposes.

1) Run-Length Matrix (RLM): The RLM $P(a, b)$ is calculated by counting the number of consecutive pixels with intensity a and length b in a specified direction. Let N be the number of gray levels.

$$P(a, b) = \sum_{x=1}^{N} \sum_{y=1}^{M} \delta(I(x, y) = i \text{ and } R(x, y) = j)$$

Normalized Gray-Level Run-Length Matrix (NGLRLM):

Normalize the RLM to obtain the NGLRLM:

$$P_{norm}(a, b) = \frac{P(a, b)}{\sum_{x=1}^{N} \sum_{y=1}^{M} P(a, b)}$$

2) Gray-Level Run-Length Matrix (GLRLM) Features: Several statistical measures can be computed from the GLRLM to extract features. Some of significant features are given below:

Short Run Emphasis (SRE):

$$SRE = \frac{\sum_{i=1}^{N} \sum_{j=1}^{M} \frac{P(a,b)}{j^2}}{\sum_{i=1}^{N} \sum_{j=1}^{M} P(a, b)}$$

Long Run Emphasis (LRE):

$$LRE = \frac{\sum_{i=1}^{N} \sum_{j=1}^{M} P(a, b) \cdot j^2}{\sum_{i=1}^{N} \sum_{j=1}^{M} P(a, b)}$$

Gray-Level Non-Uniformity (GLN):

$$\sum_{i=1}^{N} \sum_{j=1}^{M} P(a, b)^2$$

Run Length Non-Uniformity (RLN):

$$\sum_{i=1}^{N} \sum_{j=1}^{M} P(a, b)^2$$

F. U-Net Architecture

It is used for segmentation of cancer cells in given dataset images. The architecture consists of a contracting path, a bottleneck, and an expansive path.

1) Contracting path: It is responsible for capturing context and reducing the spatial resolution of the input image.

$$\text{Conv}(x, \text{filters}, \text{kernel}_{\text{size}}, \text{activation} = '\text{relu}', \text{padding} = '\text{same}'$$

x is the input tensor.

filters is the number of filters in the convolutional layer.

$\text{kernel}_{\text{size}}$ is the size of the convolutional kernel.

activation is the activation function, typically ReLU.

padding is set to 'same' to maintain the spatial dimensions.

$$\text{maxpool}(x, \text{pool}_{\text{size}}, \text{strides}$$

where,

$\text{pool}_{\text{size}}$ is the size of pooling window.

Strides is the stride of the pooling operation.

2) Skip connections: In order to concatenate feature mappings from the contracting path to the appropriate layer in the expansive path, the U-Net design uses skip connections.

$$\text{concatenate}(\text{conv}_{\text{block}_{\text{output}}}, \text{corresponding}_{\text{conv}_{\text{block}_{\text{output}}}})$$

3) Output layer: It is also a convolutional layer with a sigmoid activation function, producing the final segmentation map.

$$\text{conv}(x, 1, 1, \text{activation} =' \text{sigmoid}')$$

where:

1 is the number of filters (assuming binary segmentation, i.e., cancer cell or background).

1 x 1 convolutional kernel is used.

IV. Extreme Gradient Boosting (XGBoost)

In this paper, the Extreme Gradient Boosting (XGBoost) approach is used for the classification of input cancer and non-cancer images. Usually, a binary classification model with the target variable being a binary value indicating whether or not a patient has liver cancer is used to identify liver cancer using XGBoost. The two components of the XGBoost objective function are the regularization term, which penalizes the model's complexity in order to prevent over fitting, and the loss function, which calculates the difference between the true and predicted values.

$$\text{Objective} = \sum_{i=1}^{n} \text{loss}(y_i, \hat{y}_i) + \sum_{k=1}^{K} \Omega\,(f_k)$$

n -total training samples

y_i -True table for i^{th} sample.

$\hat{y}_i$ -predicted output for i^{th} sample.

K- Total trees ensemble.

$\Omega(f_k)$ Regularization term for the k^{th} tree.

1) Loss Function: In this scenario, the loss function which is used for classification of cancer images is logistic loss:

$$\text{loss}(y_i, \hat{y}_i) = -[y_i \log(\hat{y}_i) + (1 - y_i) \log(1 - \hat{y}_i)]$$

y_i is the true label.

$\hat{y}_i$ Predicted probability of class 1.

2) Regularization term: These terms are used by XGBoost to regulate the total model's complexity as well as the complexity of each individual tree. The regularization term for the k^{th} tree is a sum of the leaf scores:

$$\Omega(f_k) = \gamma T + \frac{1}{2} \lambda \sum_{j=1}^{T} w_j^2$$

T total leaves in the tree.

w_j score associated with the j-th leaf.

γ and λ Regularization parameters.

3) Tree Building Process: XGBoost builds trees in an additive manner, where each new tree is trained to correct the errors of the combined existing ensemble. The update at each step is given by:

$$\hat{y}_i^{(t+1)} = \hat{y}_i^{(t)} + \eta \cdot f_t(x_i)$$

The final equation classifies the input liver sample as tumor affected or not. The final architecture is given in Fig. 4 with step-by step approaches used to obtain the better output.

V. Performance Metrics

This section focuses mainly on showing the effectiveness of the proposed approach based on the outcomes. The performance metrics are obtained by using the proposed approach. The count values are obtained by the proposed classification approach. XGBoost is the classification model implemented by using the Python language with potential libraries. There are several libraries that help provide accurate results with the particular libraries. The performance is measured by using the following metrics. The count values are measured from the proposed approach. Fig. 6 shows the attributes of performance measures based on confusion matrix.

$$\text{Precision} = \frac{TP}{TP + FP}$$

$$\text{Accuracy} = \frac{TP + TN}{TP + TN + FP + FN}$$

$$\text{Recall} = \frac{TP}{TP + FN}$$

$$\text{Specificity} = \frac{TN}{TN + FP}$$

$$F1 - \text{Score} = 2 * \frac{(\text{Precision} * \text{Recall})}{(\text{Precision} + \text{Recall})}$$

A. Experimental Results

This section mainly focused on analyzing the performance of the proposed approach is compared with several existing models. This section focused on providing the analysis of every parameter that shows the huge impact on output. It includes the training and testing loss and training and testing accuracy for the given pre-trained model. Also, this consists of comparative performances of several existing algorithms compared with the proposed algorithm.

The training loss measures the performance of model on training data. It initializes the error between the estimated output and original output at the time of training phase. In this paper, the loss is minimized by updating the model parameters by using several optimization algorithms. Testing loss mainly

generalizes the model performance on new and unknown data. It is evaluated on a different dataset that the model has not seen during training. The proposed model shows the better performance by showing the balanced outcomes. The performance metrics based on the reduced testing and training loss are displayed in Fig. 7. It shows the proportion of successfully predicted instances to all instances in the dataset and is commonly stated as a percentage. There are two main types of accuracy: training and testing accuracy. Training accuracy gives an indication of how well the model has learned the training data. High training accuracy does not, however, guarantee that the model will perform well when applied to novel or unidentified data. The model's accuracy on a different dataset that it was not exposed to during training is known as testing accuracy. Since testing accuracy shows how well the model is likely to function on unknown data, it is a more significant parameter. Fig. 8 shows the performance of training phase testing phase.

Table I shows the performance of ML algorithms without using any ensemble techniques or pre-trained models. It is the classification models obtained by the implementation of ML algorithms. Fig. 9 shows the comparisons between ML algorithms.

B. Figures and Tables

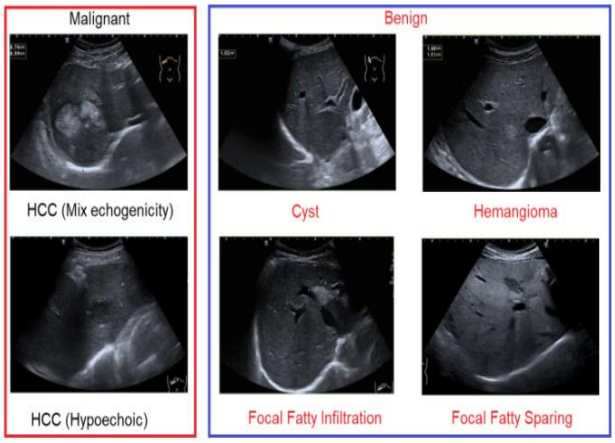

Fig. 1. Sample liver lesions.

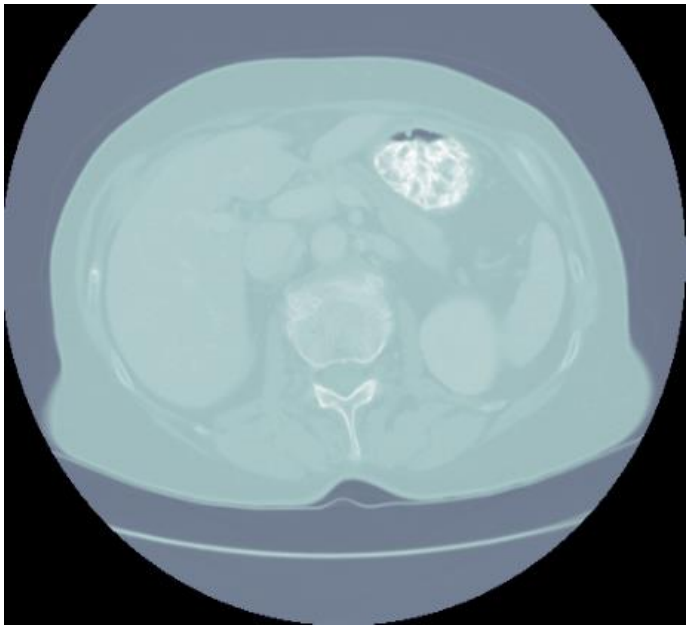

Fig. 2. Liver cancer CT scan image from dataset.

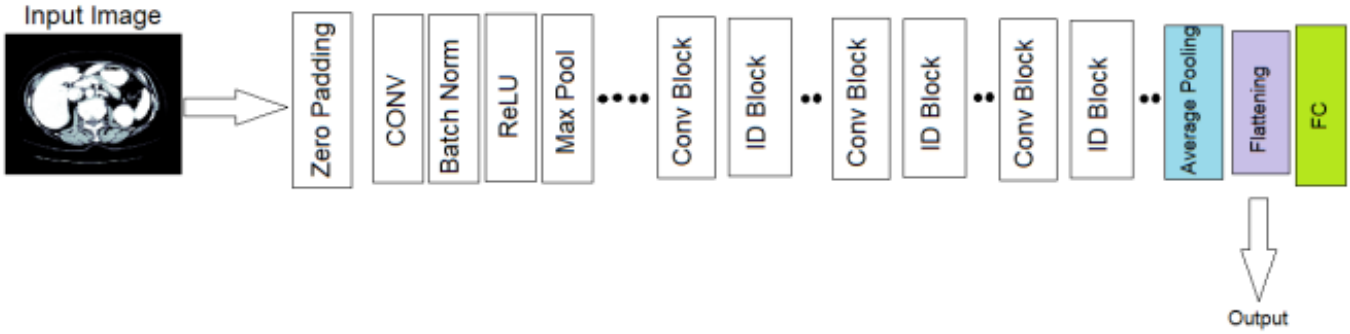

Fig. 3. Architecture of RESNET50.

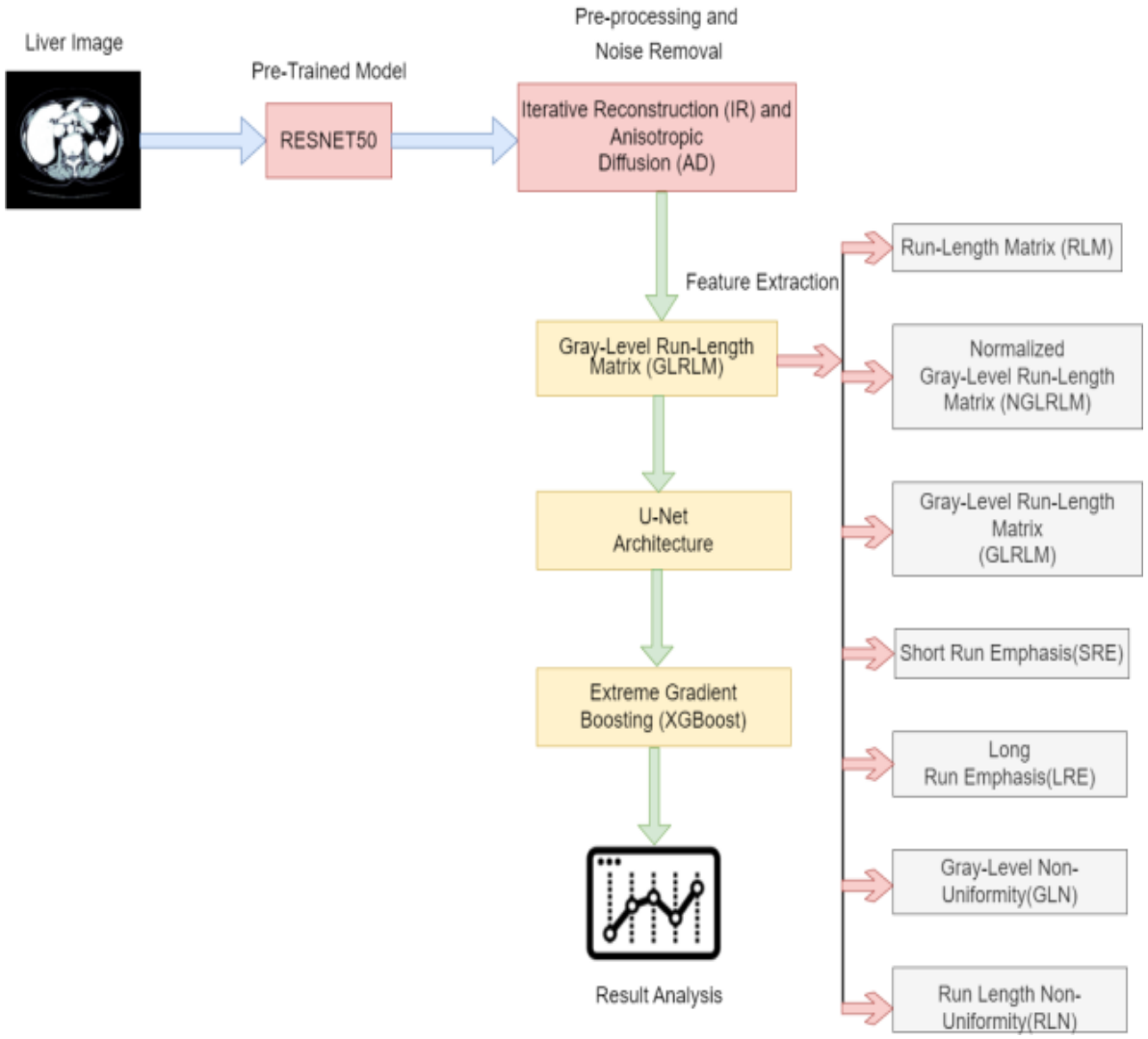

Fig. 4. The proposed architecture.

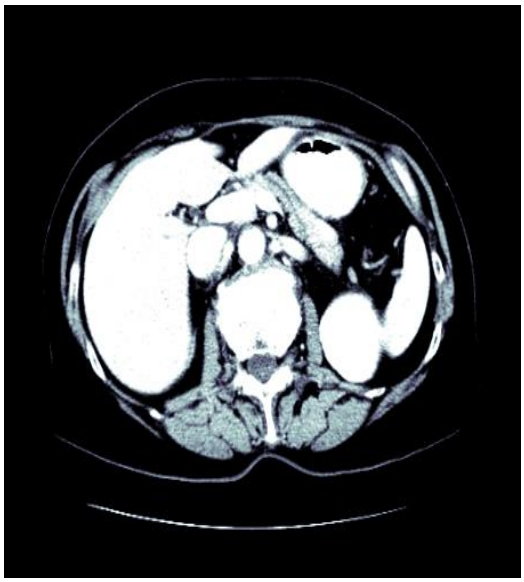

Fig. 5. The output after the Preprocessing technique.

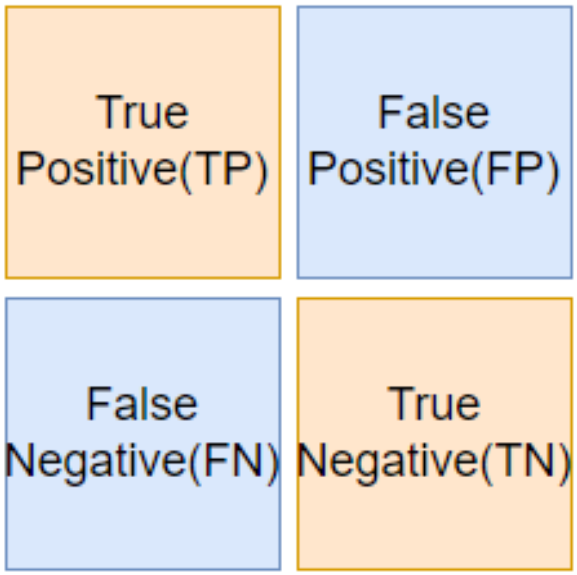

Fig. 6. Confusion matrix.

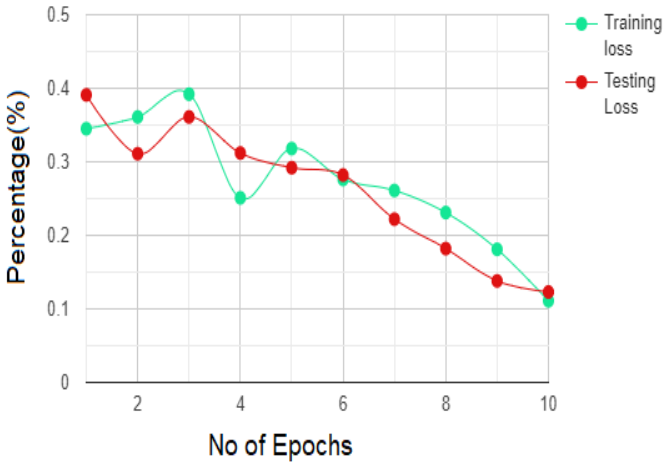

Fig. 7. Performance in terms of proposed pre-trained model.

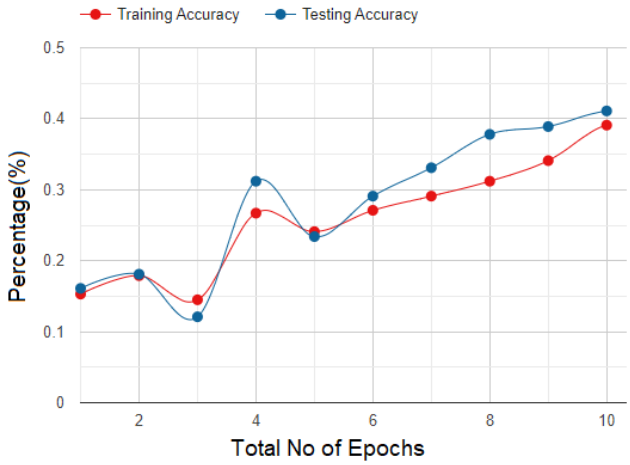

Fig. 8. The performance of pre-trained model in terms of training and testing accuracy.

TABLE I. THE PERFORMANCE OF VARIOUS ML MODELS

Parameters	Random Forest (RF)	CNN	XGBoost
Precision	73.23	76.23	86.56
Accuracy	74.53	80.34	88.12
Recall	75.12	81.23	89.23
Specificity	71.23	83.56	90.34
F1-Score	73.34	84.23	91.34

Table I shows the obtained results that are obtained by using existing algorithms such as RF, CNN and XGBoost. Among all these algorithms the XGBoost gained the better classification results compared with existing approaches. The traditional XGBoost obtained the high performance in terms of accuracy of 88.12%, precision of 86.56%, recall of 89.23, Specificity of 90.23 and F1-Score of 91.34.

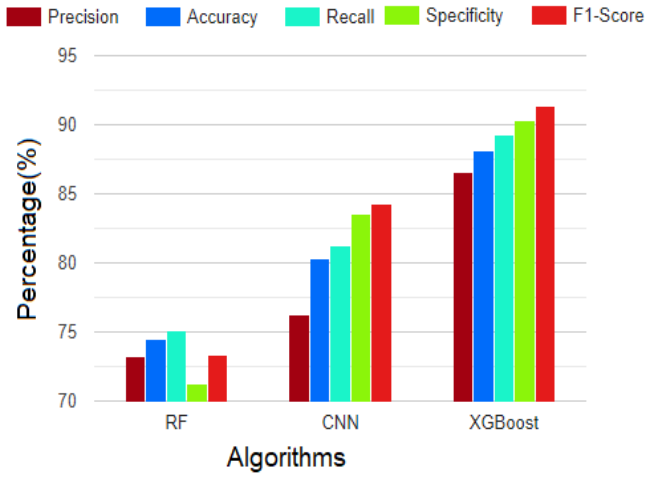

Fig. 9. The comparative performances of various ML algorithms.

TABLE II. THE OVERALL PERFORMANCE OF ALL THE ADVANCED ALGORITHMS THAT EVERY ALGORITHM IS COMBINED WITH VARIOUS PREPROCESSING AND FEATURE EXTRACTION TECHNIQUES

Parameters	Random Forest (RF)	CNN	Combined Ensemble model (CEM)
Precision	83.45	88.23	97.81
Accuracy	84.23	89.34	98.48
Recall	85.12	90.23	98.65
Specificity	81.23	90.56	98.45
F1-Score	82.87	91.23	98.19

Table II shows the comparison between traditional and Ensemble Algorithms that shows the high performance in terms of various parameters. The proposed CEM is the ensemble algorithm that combines with the U-Net and XGBoost. It achieved the high accuracy of 98.48% based on correctly classified outcomes. The remaining parameters are also shows the high rate. Finally, Fig. 10 shows the overall performances of existing and proposed algorithms.

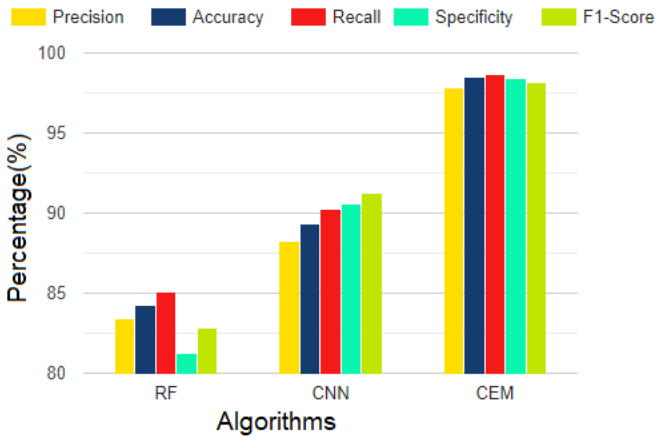

Fig. 10. The overall performances of existing and latest algorithms.

VI. CONCLUSION

In this work, we looked into the use of a Combined Ensemble Model (CEM) in liver cancer diagnosis. Utilizing each model's unique characteristics to improve overall forecast accuracy and reliability was the main goal. Our results show that the CEM technique has the potential to enhance liver cancer diagnostic skills. The ensemble model performed better than the individual models alone. It was created by combining many algorithms, such as [list of individual models]. By combining several algorithms, the constraints of using a single model were effectively mitigated and a more reliable and accurate prediction of liver cancer was made. Furthermore, the CEM demonstrated enhanced generalization capabilities, suggesting its potential applicability to diverse patient populations and datasets. The ensemble approach not only improved sensitivity and specificity but also provided a more comprehensive understanding of the complex patterns within the data. While the CEM outperformed individual models, it is crucial to acknowledge the importance of continuous refinement and optimization. Future work should focus on fine-tuning the ensemble model, exploring additional algorithms, and incorporating new features to further enhance its diagnostic capabilities. The implications of our study extend beyond the realm of liver cancer diagnosis. The success of the CEM approach highlights the value of ensemble techniques in medical decision-making, emphasizing the significance of model diversity and collaboration. This research contributes to the growing body of evidence supporting the use of ensemble models in healthcare applications. Finally, the Combined Ensemble Model presents a promising avenue for improving the accuracy and reliability of liver cancer diagnosis. As we move forward, it is essential to continue refining and validating the model on larger and more diverse datasets, ultimately paving the way for its potential integration into clinical practice.

REFERENCES

[1] Facts Figures American Cancer Society, Atlanta, GA, USA, 2018.

[2] M. U. Rehman et al., "A Novel Chaos-Based Privacy-Preserving Deep Learning Model for Cancer Diagnosis," in IEEE Transactions on Network Science and Engineering, vol. 9, no. 6, pp. 4322-4337, 1 Nov.-Dec. 2022, doi: 10.1109/TNSE.2022.3199235.

[3] A. Imran, A. Nasir, M. Bilal, G. Sun, A. Alzahrani and A. Almuhaimeed, "Skin Cancer Detection Using Combined Decision of Deep Learners," in IEEE Access, vol. 10, pp. 118198-118212, 2022, doi: 10.1109/ACCESS.2022.3220329.

[4] A. Afroz, R. Zia, A. O. Garcia, M. U. Khan, U. Jilani and K. M. Ahmed, "Skin lesion classification using machine learning approach: A survey", Proc. Global Conf. Wireless Opt. Technol. (GCWOT), pp. 1-8, Feb. 2022.

[5] M. Sattar and A. Majid, "Lung cancer classification models using discriminant information of mutated genes in protein amino acids sequences", Arabian J. Sci. Eng., vol. 44, no. 4, pp. 3197-3211, Apr. 2019.

[6] O. Ozdemir, R. L. Russell and A. A. Berlin, "A 3D Probabilistic Deep Learning System for Detection and Diagnosis of Lung Cancer Using Low-Dose CT Scans," in IEEE Transactions on Medical Imaging, vol. 39, no. 5, pp. 1419-1429, May 2020, doi: 10.1109/TMI.2019.2947595.

[7] Song-Tran Toan, Cheng Ching-Hwa and Liu Don-Gey, A multiple layer U-Net, Un-Net, for liver and liver tumor segmentation in CT, IEEE Access 9 (2020), 3752–3794.

[8] Dong Xin, Zhou Yizhao, Wang Lantian, Peng Jingfeng, Lou Yanbo and Fan Yiqun, Liver cancer detection using fully convolutional neural network based on deep learning framework, IEEE Access 8 (2020), 129889–129898.

[9] Bai Zhiqi, Jiang Huiyan, Li Siqi and Yao Yu-Dong, Liver tumor segmentation based on multi scale candidate generation and fractal residual network, IEEE Access 7 (2019), 82122–82133.

[10] Hemalatha V. and Sundar C., Automatic liver cancer detection in abdominal liver images using soft optimization techniques, Journal of Ambient Intelligence and Humanized Computing 12(5) (2021), 4765–4774.

[11] Tang Wei, Zou Dongsheng, Yang Su, Shi Jing, Dan Jingpei and Song Guowu, A two-stage approach for automatic liver segmentation with Faster R-CNN and DeepLab, Neural Computing and Applications 32(2) (2020), 6769–6778.

[12] S. Kim and J. Park, "Hybrid Feature Selection Method Based on Neural Networks and Cross-Validation for Liver Cancer With Microarray," in IEEE Access, vol. 6, pp. 78214-78224, 2018, doi: 10.1109/ACCESS.2018.2884896.

[13] M. Ahmad et al., "Deep Belief Network Modeling for Automatic Liver Segmentation," in IEEE Access, vol. 7, pp. 20585-20595, 2019, doi: 10.1109/ACCESS.2019.2896961.

[14] L. Balagourouchetty, J. K. Pragatheeswaran, B. Pottakkat and G. Ramkumar, "GoogLeNet-Based Ensemble FCNet Classifier for Focal Liver Lesion Diagnosis," in IEEE Journal of Biomedical and Health Informatics, vol. 24, no. 6, pp. 1686-1694, June 2020, doi: 10.1109/JBHI.2019.2942774.

[15] Yamakawa M, Shiina T, Nishida N, Kudo M (2019) Computer aided diagnosis system developed for ultrasound diagnosis of liver lesions using deep learning. IEEE International Ultrasonics Symposium, IUS 2019-Octob, pp 2330–2333.

[16] Aslam, M.S.; Younas, M.; Sarwar, M.U.; Shah, M.A.; Khan, A.; Uddin, M.I.; Ahmad, S.; Firdausi, M.; Zaindin, M. Liver-Tumor detection using CNN ResUNet. Comput. Mater. Contin. 2021, 67, 1899–1914.

[17] Piyush Kumar Shukla, Mohammed Zakariah, Wesam Atef Hatamleh, Hussam Tarazi, Basant Tiwari, "AI-DRIVEN Novel Approach for Liver Cancer Screening and Prediction Using Cascaded Fully Convolutional Neural Network", Journal of Healthcare Engineering, vol. 2022, Article ID 4277436, 14 pages, 2022.

[18] Sanyal AJ, Williams SA, Lavine JE, Neuschwander-Tetri BA, Alexander L, Ostroff R, Biegel H, Kowdley KV, Chalasani N, Dasarathy S, Diehl AM, Loomba R, Hameed B, Behling C, Kleiner DE, Karpen SJ, Williams J, Jia Y, Yates KP, Tonascia J. "Defining the serum proteomic signature of hepatic steatosis, inflammation, ballooning and fibrosis in non-alcoholic fatty liver disease." J Hepatol. 2023 Apr;78(4):693-703. doi: 10.1016/j.jhep.2022.11.029.

[19] Fu Y, Zhou Y, Shen L, Li X, Zhang H, Cui Y, Zhang K, Li W, Chen WD, Zhao S, Li Y, Ye W. Diagnostic and therapeutic strategies for non-alcoholic fatty liver disease. Front Pharmacol. 2022 Nov 2;13:973366. doi: 10.3389/fphar.2022.973366.

[20] Zhou JH, Cai JJ, She ZG, Li HL. Noninvasive evaluation of nonalcoholic fatty liver disease: Current evidence and practice. World J Gastroenterol. 2019 Mar 21;25(11):1307-1326. doi: 10.3748/wjg.v25.i11.1307.

[21] Marengo A, Rosso C, Bugianesi E. Liver cancer: connections with obesity, fatty liver, and cirrhosis. Annu Rev Med (2016) 67:103–17. doi: 10.1146/annurev-med-090514-013832.

[22] Ou-Yang MC, Sun Y, Liebowitz M, et al. Accelerated weight gain, prematurity, and the risk of childhood obesity: a meta-analysis and systematic review. PLoS One. 2020;15(5):e0232238.

[23] Kwon J and Choi K 2020 Trainable multi-contrast windowing for liver CT segmentation Proc. - 2020 IEEE Int. Conf. Big Data Smart Comput. BigComp 2020 169–72.

[24] Manjunath, R.V., Ghanshala, A. & Kwadiki, K. Deep learning algorithm performance evaluation in detection and classification of liver disease using CT images. Multimed Tools Appl (2023). https://doi.org/10.1007/s11042-023-15627-z..

[25] B. Lakshmipriya, Biju Pottakkat, G. Ramkumar, "Deep learning techniques in liver tumour diagnosis using CT and MR imaging - A systematic review", Artificial Intelligence in Medicine, Volume 141, 2023, https://doi.org/10.1016/j.artmed.2023.102557.

[26] Piyush Kumar Shukla, Mohammed Zakariah, Wesam Atef Hatamleh, Hussam Tarazi, Basant Tiwari, "AI-DRIVEN Novel Approach for Liver Cancer Screening and Prediction Using Cascaded Fully Convolutional Neural Network", Journal of Healthcare Engineering, vol. 2022.

[27] Heng Zhang, Kaiwen Luo, Ren Deng, Shenglin Li, Shukai Duan, "Deep Learning-Based CT Imaging for the Diagnosis of Liver Tumor", Computational Intelligence and Neuroscience, vol. 2022.

[28] Liping Liu, Lin Wang, Dan Xu, Hongjie Zhang, Ashutosh Sharma, Shailendra Tiwari, Manjit Kaur, Manju Khurana, Mohd Asif Shah, "CT Image Segmentation Method of Liver Tumor Based on Artificial Intelligence Enabled Medical Imaging", Mathematical Problems in Engineering, vol. 2021.

[29] Nayantara, P Vaidehi et al. “Computer-aided diagnosis of liver lesions using CT images: A systematic review.” Computers in biology and medicine vol. 127 (2020): 104035. doi:10.1016/j.compbiomed.2020.104035.

[30] Zhang, G., Yang, Z., Gong, L., Jiang, S., Wang, L., Cao, X., Wei, L., Zhang, H., & Liu, Z. (2019). An Appraisal of Nodule Diagnosis for Lung Cancer in CT Images. Journal of medical systems, 43(7), 181. https://doi.org/10.1007/s10916-019-1327-0.

[31] Mubashir Ahmad, Syed Furqan Qadri, M. Usman Ashraf, Khalid Subhi, Salabat Khan, Syeda Shamaila Zareen, Salman Qadri, "Efficient Liver Segmentation from Computed Tomography Images Using Deep Learning", Computational Intelligence and Neuroscience, vol. 2022.

[32] S. Manoj Kumar, V. Anbu, S. K. Abishek, N. Jeevanantham and H. Ashwin Kumar, "Prediction Of Liver Disease Using Statistical Machine Learning Methods," 2023 International Conference on Computer Communication and Informatics (ICCCI), Coimbatore, India, 2023, pp. 1-6, doi: 10.1109/ICCCI56745.2023.10128370.

[33] X. Li, H. Chen, X. Qi, Q. Dou, C.-W. Fu, and P.-A. Heng, "H-DenseUNet: Hybrid densely connected UNet for liver and tumor segmentation from CT volumes," IEEE Trans. Med. Imag., vol. 37, no. 12, pp. 2663–2674, Dec. 2018.

[34] Amita Das, U. Rajendra Acharya, Soumya S. Panda, Sukanta Sabut, "Deep learning based liver cancer detection using watershed transform and Gaussian mixture model techniques", Cognitive Systems Research, Volume 54, 2019.

[35] D. Anandan, S. Hariharan, and R. Sasikumar. 2023. "Deep learning based two-fold segmentation model for liver tumor detection". J. Intell. Fuzzy Syst. 45, 1 (2023), 77–92. https://doi.org/10.3233/JIFS-230694.